Construction and Building Materials 347 (2022) 128597

Contents lists available at ScienceDirect

Construction and Building Materials

journal homepage: www.elsevier.com/locate/conbuildmat

Durability and microstructural analyses of concrete produced with treated demolition waste aggregates

Qusai Al-Waked *, Jiping Bai, John Kinuthia, Paul Davies

Faculty of Computing, Engineering and Science, University of South Wales, Treforest Campus CF37 1DL, UK

ARTICLE INFO

Keywords:
Recycled aggregate
Freeze-thaw
Sulphate attack
Microstructure
Scanning electron microscopy (SEM)
Cost analysis

ABSTRACT

The incorporation of recycled aggregate (RA) from the construction and demolition waste (C&DW) in civil engineering applications has become a hot research topic worldwide due to the associated environmental benefits of its application. Nonetheless, the poor quality of RA reduced its attraction to be utilized widely in the construction industry. This research examined the effects of soaking RA in cement-pulverized fuel ash-silica fume method (SCP), sand envelope mixing approach (SE), and bi-combination of SCP + SE on the water absorption, resistance to freeze–thaw, and sulphate resistance of recycled aggregate concrete (RAC). This study also investigated the microstructure of the enhanced RACs using scan electron microscopy (SEM) images to validate the experimental results. In addition, a detailed cost analysis of the different enhancement methods utilized in this study was carried out. The enhanced RACs demonstrated improved durability performance which was confirmed by the SEM images. This was ascribed to the strengthened interfacial transition zone, strengthened adhered mortar, better overall interlocking of the treated RA with the new cement paste, filled-up pores and micro-cracks, reduced porosity, and compacted denser microstructure. The outcome of this study would be in a great benefit to researchers, RA producers, design engineers, and stockholders to get a better knowledge on the durability property of RAC produced with 100 % treated RA, and thus promote the use of RA in the construction industry.

1. Introduction

The activities of the construction industry generate large amounts of waste. In numerous countries, the amount of construction and demolition waste (C&DW) generated is rapidly increasing every year [1]. The dumping and landfilling of C&DW have rapidly led to a series of issues for the environment because C&DW may contain hazardous materials [2]. Although several countries recycle around 80 % of C&DW such as Japan, the Netherlands, and Germany, there are some developing countries with an average recycling rate of 20 % to 40 % [3]. Accordingly, promoting the use of recycled aggregate (RA) from the C&DW into new concrete as a replacement for natural aggregate (NA) is an essential priority. This would lead to a reduction in carbon dioxide emissions and contribute significantly towards preserving the environment by minimizing the depletion of natural resources, thus leading to a sustainable and green future [4].

Nonetheless, the poor quality of RA in terms of its engineering properties has limited its use to non-structural applications such as road bases, blinding concretes, and footpaths [5]. Extensive studies on the effects of RA on concrete properties showed that as the substitution level of RA increases the following changes to concrete properties were reported, reduction in consistency [6], decreased density [7], increase in permeability [8], poor chloride ion permeability [9], low resistance to acid and sulfate attach [9], reduction in mechanical properties [7], and decrease in elastic modulus [10]. Bahraq et al. [9] stated that the presence of the adhered mortar on RA surface is the main key affecting factor that leads to higher water absorption, lower specific gravity, and higher Los Angeles abrasion mass loss, compared to NA.

Durability of concrete can be defined as its ability to withstand various types of damage under exposure to the surrounding environment while maintaining its strength and appearance for its designed service period [11]. The high water absorption of RA and the presence of adhered mortar on the RA surface usually lead to weaker durability performance of recycled aggregate concrete (RAC) compared to natural aggregate concrete (NAC). In view of this, research to enhance the quality of RA and the engineering performance of RAC has been

Abbreviations: RA, Recycled aggregate; NA, Natural aggregate; RAC, Recycled aggregate concrete; NAC, Natural aggregate concrete; ITZ, Interfacial transition zone; SEM, Scan electron microscopy.

* Corresponding author.
E-mail address: qusai.al-waked@southwales.ac.uk (Q. Al-Waked).

https://doi.org/10.1016/j.conbuildmat.2022.128597
Received 2 June 2022; Received in revised form 18 July 2022; Accepted 25 July 2022
Available online 29 July 2022

extensively conducted over the past few decades [12,13].

The enhancement methods used to enhance RA and RAC by different researchers can be categorized into three main methods, removing the adhered mortar, strengthening the adhered mortar, and improving the whole matrix of the RAC. Removing the adhered mortar can include treatments such as mechanical grinding [13], presoaking in acid solution [12], and ultrasonic water cleaning [14]. Although these methods can offer great enhancement to the quality of RA, they may result in adverse effects on the RA. For instance, mechanical grinding could result in micro-cracks on the RA surface during the treatment process [13].

On the other hand, treatment techniques involving strengthening the adhered mortar might be of greater benefit compared to removing the adhered mortar. Strengthening the adhered mortar may include treatment techniques such as surface coating RA with pozzolan slurry [15], calcium carbonate biodeposition [16], soaking RA in sodium silicate solution [17], soaking RA in cement-pozzolan solution [18], and accelerated carbonation [19].

Improving the whole matrix of RAC can include methods such as batching techniques which are modified batching procedures that generally aim at limiting the amount of mixing water that is absorbed by RA during mixing. A few of these methods include stone envelope with pozzolanic powder [20], two-stage mixing technique [21], sand enveloped mixing approach [22], and mortar mixing approach [22].

2. Research significance

Although the literature holds a large number of studies on the effects of different enhancement methods on RA and RAC properties, the structural application of RAC is still limited due to the inferior durability properties of RAC [23]. The literature also showed scant studies are available on the effects of different treatment methods on the durability properties of RAC. The vast majority of the studies in the literature focused on recycled concrete aggregate rather than RA from the C&DW.

The quality of RA plays an important role in altering the mechanical and durability properties of RAC. To this end, this research aims at evaluating the performance of three enhancement methods, soaking RA in cement-pulverized fuel ash-silica fume solution (SCP), sand envelope mixing approach (SE), and bi-combination of these two methods, on enhancing the durability of RAC including, water absorption, resistance to freezing-thawing, and to sulphate attack.

The solution design of the SCP treatment was selected based on the optimal performance of different solutions investigated in the previous study of Al-Waked et al. [24]. Furthermore, the literature showed limited studies on the effects of SE batching technique and bi-combination of SCP and SE method on the durability properties of concrete produced with 100 % RA from construction and demolition waste.

This study also includes microstructural analyses using Scan Electron Microscopy (SEM) images to report any changes to the microstructure of RAC after the application of these enhancement methods. In addition, a comprehensive analysis of cost and other influencing factors is provided in this study for comparison purposes. Accordingly, it is anticipated that this study would undoubtedly enrich the literature and provide better understanding of the durability performance of enhanced RAC with the overall aim of expanding the application of RA in the construction industry.

3. Materials characteristics

3.1. Aggregates

20/10 mm and 10/4 mm crushed limestone aggregates (NA) were utilized throughout this study (Fig. 1a). NA conforming BS EN 12620:2002 + A1: 2008 [25] was supplied from Jewson UK Caerphilly, South Wales, UK. The recycled aggregates (RA) (Fig. 1b) used were a mix of construction and demolition waste with a clean size range of 20/10 mm and 10/4 mm confirming BS EN 13242: 2013 [26] and were processed in accordance with WRAP quality protocol [27]. The RA were supplied by Derwen Group, Neath Abbey, UK. RA consisted of different construction materials, brick, glass, bituminous, rounded stones, and recycled concrete aggregate. Table 1 shows the compositions of RA in accordance with BS 8500–2: 2015 + A2: 2019 [28]. The mechanical and physical properties of the NA and RA are provided in Table 2, while the

Table 1
Compositions of recycled aggregates in this study (BS 8500–2:2015 + A2: 2019).

	R_c (%)	R_u (%)	R_b (%)	R_g (%)	R_a (%)	X (%)
Sample 1	49.14	29.47	12.51	0.17	8.38	0.34
Sample 2	47.5	28.06	11.5	1.12	11.00	0.48
Sample 3	50.6	25.8	13.4	0.00	9.5	0.37
BS limits	–	–	–	–	≤10 %	≤1%
Mean	49.08	27.78	12.47	0.42	9.6	0.39

Notes: R_c - cement-based products, R_u - unbounded aggregates and/or natural stones, R_b - clay masonry units i.e., bricks and tiles, calcium silicate masonry unit, R_a - bituminous materials, and X - miscellaneous materials and/or non-floating wood, plastic, and rubber, R_g - crushed glass.

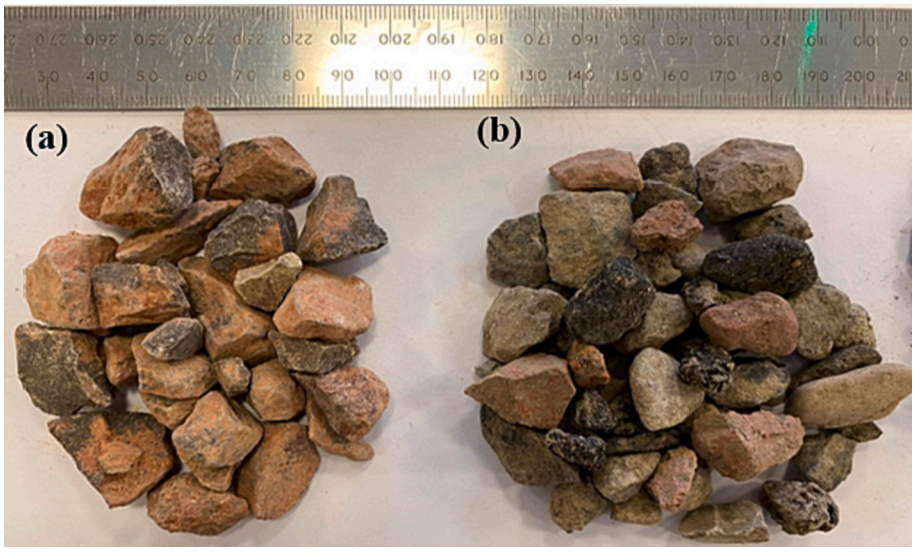

Fig. 1. Coarse aggregates used in this study (a) coarse natural aggregate, (b) coarse recycled aggregate.

Table 2
Characteristics of the RA compared with NA and relevant BS EN standards.

Characteristic	NA	RA	TRA	BS limits	Standard
Flakiness Index (%)	18	27	–	<40	BS EN 933–3:2012 [31]
Shape Index (%)	12	18	–	<55	BS EN 933–4:2008 [32]
Water Absorption (%)	1.5	6.1	3	<8	BS EN 1097–6:2013 [33]
Density kg/m^3	2480	2120	–	–	BS EN 1097–6:2013 [33]
Impact Value (%)	14	17	14.7	<32	BS EN 1097–2:2020 [34]
LA (%)	18	26	–	<50	BS EN 1097–2: 2020 [34]

Note, TRA – treated RA by soaking in cement-PFA + SF solution

particle size distribution of NA and RA in accordance with BS EN 933–1:2012 [29] is shown in Fig. 2.

As can be observed in Table 2, untreated RA showed inferior characteristics compared to NA due to the presence of the adhered mortar [23]. Nevertheless, treated RA with cement-PFA + SF solution showed enhanced Aggregate Impact Value (AIV) and Water Absorption (WA). For instance, the AIV was reduced by 13 % while the WA was reduced by 54 %. This can be attributed to the filling and sealing effect of the pozzolan used in the treatment [24].

It is thought that the source of RA plays a vital role in the quality of RA. For instance, Munir et al. [30] investigated different characteristics of RA with 5 % impurities (i.e., glass, asphalt, bricks, and ceramic) and found that the WA of RA is 6.85 % and the crushing value was 31 %. Munir et al. [30] also stressed that the treatment methods utilized such as carbonation treatment directly affects the water absorption property of RA through effectively filling or sealing the voids and pores on RA surface.

On the other hand, the crushing value or the impact value of RA is mainly controlled by several aspects, such as the strength of the parent concrete (source), and the type of crusher used on site [30]. Accordingly, this can explain the higher enhancement observed in the WA compared to the AIV after the treatment utilized in the current study.

3.2. Portland cement

A commercially available Portland cement (CEM I-42.5 N) conforming BS EN 197–1: 2011 [35] was used throughout this study. The CEM I was also supplied from Jewson UK limited, Caerphilly, South Wales, UK. The oxide and physical composition of CEM I are provided in Table 3.

3.3. Pozzolan

The pulverized fuel ash (PFA) used throughout this study compliant with BS EN 450–1:2012 [36] was sourced from a local supplier. Undensified silica fume (SF) with a commercial code 971U and 97.1 % purity conforming BS EN 13263–2:2005 + A1:2009 [37] was used throughout this study. It was manufactured by Elkem Silicon Materials, Norway.

4. Experimental program

4.1. Enhancement methods

4.1.1. Soaking RA in cement-PFA + SF solution (SCP)

The recycled aggregates were treated by soaking in Portland cement - pulverized fuel ash - silica fume solution. These pozzolan materials were selected to fulfil the environmental and economic criteria. The solution was prepared by mixing the raw materials with water for several minutes (see Table 4). Then the recycled aggregates were added to the solution and soaked for 4 hrs at a 10 % concentration level. Thereafter, the recycled aggregates were removed from the solution bath and let to drain for 10 min and then air-dried at room temperature for 24 hrs prior

Table 3
Oxide compositions and physical properties of powder materials used throughout this study.

Oxide	Composition by (wt%)		
	PC	SF	PFA
CaO	61.49	–	0.22
SiO_2	18.84	97.1	59.04
Al_2O_3	4.77	0.1	34.08
Fe_2O_3	2.87	0.2	2.00
SO_3	3.12	0.06	0.05
Na_2O	0.02	–	1.26
Physical properties			
Colour	Grey	Dark Grey	Light Grey
Bulk density (kg/m^3)	1400	120–220	800–1000
Specific gravity (Mg/m^3)	3.16	2.20	2.90

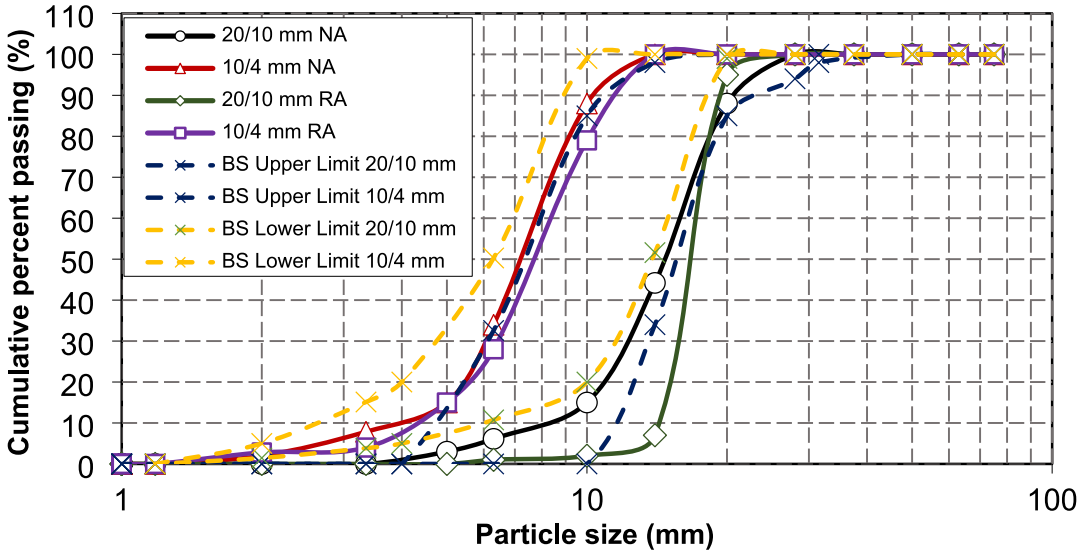

Fig. 2. Particle size distribution of coarse RA and coarse NA (BS EN 933–1:2012).

Table 4
Proportions of treatment solution for 1000 g of RA.

Treatment solution	Binder (g)			RA (g)	Water (g)	Concentration level (binder to water ratio)
	PC	PFA	SF			
PC - PFA + SF	80	60	60	1000	2000	10 %

to casting. The design of the solution compositions, selection of soaking time, and concentration level were based on several trial formulations of solutions with different concentration levels. Four hours of soaking time and 10 % solution concentration level were found to be optimal.

4.1.2. Sand envelope mixing approach (SE)

The sand was firstly mixed with 75 % of the mixing water for 30 s, cement was then added to the mixture and mixed for 45 s. Thereafter, the untreated recycled aggregate were added to the mixture with the rest of the mixing water and mixed for 90 s. This technique aimed at minimizing the amount of mixing water to be absorbed by RA during mixing.

4.1.3. Bi-combination of SCP + SE

The untreated RA were firstly dried to constant mass and then soaked in the pre-prepared cement-SF + PFA solution for 4 hrs, and then air-dried at room temperature for 3 days. Thereafter, the treated RA were incorporated into the mixing design of RAC and mixed using sand envelope batching technique.

4.2. Concrete mix design

Table 5 shows concrete mix proportions produced with the enhancement methods utilized at three different water to cement ratios, 0.4, 0.5, and 0.6.

4.3. Specimens preparation & Testing of concrete

Cube test specimens of dimension of (100 mm × 100 mm × 100 mm) were utilized in the production of all the concrete. The test specimens were prepared in accordance with BS EN 206:2013 + A1:2016 [38]. The de-moulding of the test specimens was carried out after 24 hrs of casting at room temperature, and curing done in accordance with BS EN 12390–2:2019 [39].

The assessment of the durability performance of the concrete in terms of resistance to freeze–thaw was carried out in a Prior Clave chamber LCH/600/25 model of 0.7 m^3 volume capacity, in accordance with PD CEN/TS 12390–9:2016 [40]. The test hardened concrete cube specimens were firstly left in the freezing chamber for seven days at −17 °C temperature and then thawed for 1 hr in a controlled temperature water bath set at 20 ± 2 °C. This cycle of freezing and thawing was repeated 20 times while the weight change was recorded after each cycle, and the compressive strength loss recorded after 4 and 20 cycles.

Water absorption was carried out in accordance with BS 1881–122:2011 + A1:2020 [41]. Testing for sulphate attack involved the concrete test specimens being first cured in a water bath at a controlled temperature of 20 ± 2 °C for 7 days. Seawater saline solution was selected for concrete specimen immersion. The immersion was carried out in lidded plastic containers in accordance with BS EN 206:2013 + A2: 2021 [42].

After 7 days of water curing, the concrete specimens were removed and placed into the lidded container for sulphate attack investigations. A visual inspection was undertaken to report any scaling, spalling, cracking, or chipping that occurred to any of the concrete specimens after freeze–thaw and sulphate attack tests. The microstructure investigation was carried out Using a MIRA3 TESCAN Scanning Electron Microscope (SEM), fitted with a Solid-state Backscattered (electron) Detector (SBD).

5. Results and discussion

5.1. Effects of SCP and SE on water absorption of RACs

Fig. 3 shows the results of the water absorption of the treated RACs in comparison with untreated RAC2 and NAC1 mixes, at 0.4, 0.5, and 0.6 w/c ratios. As a general trend for all the test concretes specimens, the lower the w/c ratio the lower was the water absorption.

NAC1 mixes recorded the lowest water absorption values across all the test concrete mix specimens, at all w/c ratios, whilst RAC2 mixes exhibited the highest water absorption values at all w/c ratios. It can also be seen that all the treatment methods varied in the enhancement of the water absorption of RAC.

The bi-combination of soaking RA in cement-PFA + SF prior to mixing and batching using the sand envelope mixing approach, presented in SCP + SE mixes, produced the highest enhancement in water absorption.

The water absorption of a given test concrete specimen reflects on its porosity state, hence the higher the porosity of concrete, the higher its water absorption property [43]. The water absorption for all the designed concrete in general increased with an increase in w/c ratio. This is mainly ascribed to the increased pores and voids and lesser dense microstructure of lower strength concrete. This is in line with the work of Thomas et al. [44] who stated that higher-strength concrete tends to show lower water absorption compared to concrete of lower-strength. According to Lotfi et al. [45], designing concrete with a low water/

Table 5
Concrete mix proportion for various RAC produced with different enhancement methods.

Specimen designation	PC (kg/m^3)	Water (kg/m^3)	w/c ratio	NA (kg/m^3)	RA (kg/m^3)	FA (kg/m^3)	Mixing method	Notes
W040/NAC1	450	180	0.4	1257	0	677	NMA	NAC (control 1)
W040/RAC2	450	180	0.4	0	1257	677	NMA	Un-treated RAC (control 2)
W040/SCP	450	180	0.4	0	1257	677	NMA	Soaking RA in PC-SF + FA solution
W040/SE	450	180	0.4	0	1257	677	SE	Untreated RA
W040/SCP + SE	450	180	0.4	0	1257	677	SE	Soaking RA in PC-SF + FA solution
W050/NAC1	350	175	0.5	1257	0	677	NMA	NAC (control 1)
W050/RAC2	350	175	0.5	0	1257	677	NMA	Un-treated RAC (control 2)
W050/SCP	350	175	0.5	0	1257	677	NMA	Soaking RA in PC-SF + FA solution
W050/SE	350	175	0.5	0	1257	677	SE	Untreated RA
W050/SCP + SE	350	175	0.5	0	1257	677	SE	Soaking RA in PC-SF + FA solution
W060/NAC1	250	150	0.6	1257	0	677	NMA	NAC (control 1)
W060/RAC2	250	150	0.6	0	1257	677	NMA	Un-treated RAC (control 2)
W060/SCP	250	150	0.6	0	1257	677	NMA	Soaking RA in PC-SF + FA solution
W060/SE	250	150	0.6	0	1257	677	SE	Untreated RA
W060/SCP + SE	250	150	0.6	0	1257	677	SE	Soaking RA in PC-SF + FA solution

NMA – normal mixing approach/ conventional mixing, SE – sand envelope mixing approach, FA – fine aggregate, NA – natural aggregate, NAC – natural aggregate concrete.

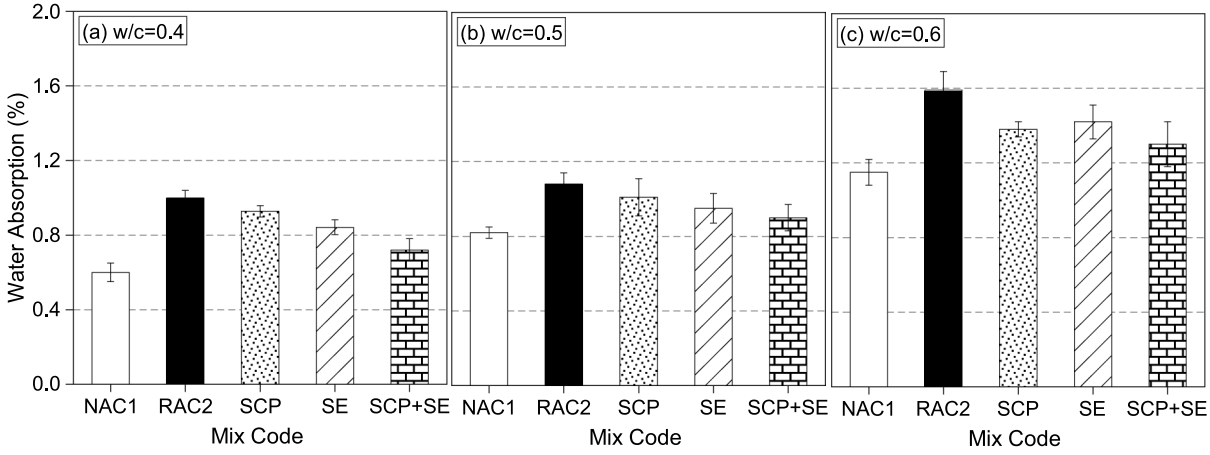

Fig. 3. Results of the water absorption of the treated RACs in comparison with RAC2 and NAC1.

cement ratio and higher cement content reduces the capillary voids, and thus a reduction in the water absorption can be achieved. The current test results showed higher water absorption of the untreated RAC2 mixes compared to NAC1 mixes, this is because of the porous nature of RA given to the attached adhered mortar around the RA surface which consists of micro-cracks and pores that are formed during the preparation of RA.

Similar observations were given in the study of Debieb et al. [46] who argued that the water absorption of RAC is significantly lower than that of NAC by 0.4 % to 0.6 %. Kwan et al. [47] stated that due to the porous nature of RA and the developed micro-cracks during the crushing process, its incorporation in concrete significantly increases the permeability.

Lotfi et al. [45] stated that the adverse effects of RA on the high water absorption of the RAC can be mitigated by utilizing lower water to binder ratio. Tam & Tam [48] stressed that mixing RAC using batching approach increase the RAC resistance to water absorption due to the reduced water absorption. In this study, the enhanced water absorption by SE mixes using the SE method (sand enveloped mixing approach) can be ascribed to the process of the SE mixing approach, in which the RA is covered with premixed cement/ mortar slurry that filled up the cracks and pores of RAC, hence enhancing its resistance to water absorption [49].

The enhanced water absorption provided by the SCP mixes (soaking RA in cement-PFA + SF solution) can be explained by the formation of a thin coated pozzolanic layer that blocked the pores and micro-cracks, thus enhancing the ITZ of RA, and lowering the porosity of RAC [21].

5.2. Effects of SCP and SE on resistance to freeze–thaw cycles of RACs

5.2.1. Visual inspection

Table 6 shows the description of defect/damage endured by the different concrete mixes after visual inspection after the freezing and thawing repeated cycles. Fig. 4 shows some of the test specimens after 20 successive freeze–thaw cycles. As a general trend, the visual inspection showed the damage/ defect phenomena of the RAC2 specimens were similar to those of the NAC1 specimens, but the extent and degree of the damage were different. At the end of the 20th freeze–thaw cycle, all the concrete specimens experienced chipping and scaling, the intensity of chipping and scaling was being more prominent with increase in w/c ratio and increase in freeze–thaw cycles.

5.2.2. Mass change due to freeze–thaw cycles

A typical profile of the effects of freezing and the thawing cycles on the mass change of the NAC1, RAC2 and the enhanced RAC specimens is shown in Fig. 5.

At the start of the freezing and thawing cycles, all the concrete specimens showed mass gain regardless of the w/c ratio, with no further mass gain after the 4th and 6th cycles. This can be explained by the filling of the enclosed pores with water within the concrete matrix caused by the freezing action of water. At the end of the 6th cycle, the highest mass gain was observed for RAC2 specimens across all the concrete specimens, whilst the lowest recorded mass gain was for the NAC1 specimens. This is in line with the study of Salem et al. [50] who stated that the higher mass gain of the untreated RAC2 specimens at the start of the freeze–thaw cycles can be ascribed to the penetrated water into the inner cracks and pores of the RAC after exposure to freeze–thaw filling all the pores and interfacial transition zone (ITZ). The enhanced RAC specimens given in SCP, SE, and SCP + SE mixes showed reductions in mass gain compared to the RAC2 specimens. This can be ascribed to the enhanced water absorption of RAC after these enhancement methods.

A general trend of mass loss occurred after around 4 to 6 freeze–thaw cycles for all the concrete specimens, and the degree of the mass loss increased with increase in w/c ratio and increased in the freezing and thawing cycles. This is attributed to the higher number of capillary

Table 6
Description of the visual inspection of damage/defects endured by the different concrete cube specimens during and at the end of the freeze and thaw cycles.

Description of Damage	Visual Remarks
Fractures	No fractures were encountered for all the concrete specimens investigated after the end of the 20th freeze–thaw cycle.
Scaling/ Peeling	Minimal scaling was observed on all the NAC1 specimens during and after the end of the freeze–thaw cycles. RAC2 specimens exhibited prominent scaling after the 8th freeze–thaw cycle. The treated RAC specimens experienced minor to medium scaling on all the concrete cubes faces during the freeze–thaw cycles.
Hairline Cracks < 0.2 mm	No hairline cracks were noticed on any of the concrete test specimens throughout the freeze–thaw cycles.
Surface Crack > 0.2 mm	No surface cracks were observed on any of the concrete specimens throughout the freeze–thaw cycles up to 20 cycles.
Chipping	Chipping of concrete edges was observed on all the concrete specimens throughout the freeze–thaw cycles. Minor chippings were observed on the NAC1 specimens, whilst the RAC2 specimen exhibited prominent chippings along its edges. Treated RAC specimens showed somewhat minor chippings along the edges throughout the freeze–thaw cycles.
Craters	Visual inspections showed no craters in any of the concrete specimens throughout the freeze–thaw cycles.
Major Spalling/ Delamination	Observations showed no major spalling nor delamination occurred on any of the concrete specimens during the freeze–thaw cycles.

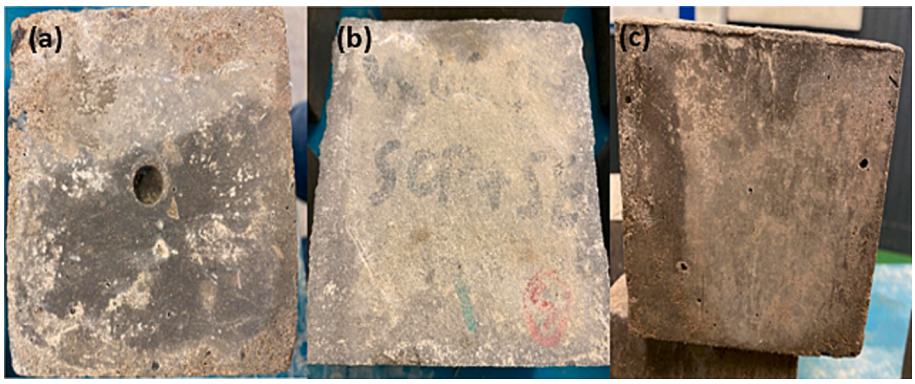

Fig. 4. Concrete cube test specimens after 20 successive freeze–thaw cycles, (a) RAC2 specimen, (b) SCP + SE specimen, (c) NAC1 specimen.

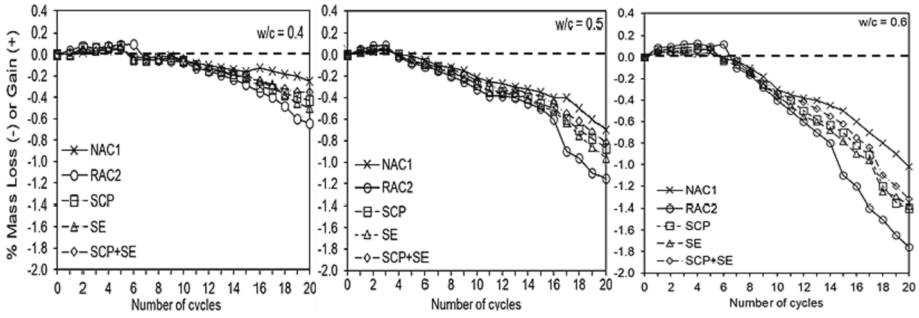

Fig. 5. Mass change (Loss or gain) due to freeze–thaw cycles.

pores, average aperture and porosity of higher w/c ratios. The NAC1 specimens recorded the lowest mass loss across all the concrete specimens after the end of the 20th freezing and thawing cycles. Whereas the RAC2 specimens experienced the highest mass loss.

This is mainly attributed to the high water absorption of RA which can drain into the cement paste and then lead to more intense frost damage. The absorbed water within the concrete matrix gets frozen upon exposure to freeze–thaw cycles, leading to internal cracks and pressure, hence resulting in the spalling of mortar and loss of mass [51]. Wu et al. [52] concluded that the RAC specimens endured lower resistance to freeze and thaw cycles in terms of mass loss, compared to NAC specimens due to internal cracks developed and pressure endured. This is also in line with the work of Kazmi et al. [51] who stated that the higher mass loss for RAC specimens is ascribed to the additional pores of RAC compared to NAC, which results in a rise in the water ingress through these pores leading to further internal pressure and micro-cracks of RAC.

All the treated RAC specimens showed a reduction in mass loss compared to RAC2 mixes. Among all the treated RAC specimens, the SCP + SE mixes showed the lowest mass loss. This is mainly attributed to the strengthening of the attached adhered mortar via these treatments, which resulted in reduced porosity, lesser cracks and denser microstructure of the enhanced RAC specimens [51]. It should be noted that scant studies are available on the effects of treatment methods on the resistance to freeze–thaw of RAC.

5.2.3. *Strength loss due to freeze–thaw cycles*

Fig. 6 shows the effects of freezing and thawing cycles on the compressive strength of the NAC1 specimens, RAC2 specimens and the treated RAC specimens at 4 weeks and 20 weeks.

Observations showed a general trend of strength loss across all the concrete specimens after 4 weeks of freeze–thaw cycles. The strength

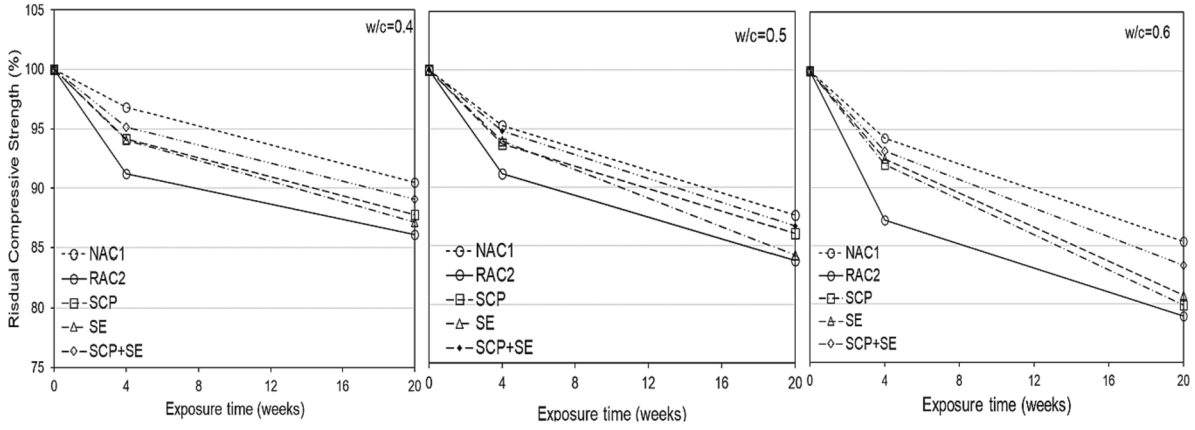

Fig. 6. Residual compressive strength of the different concretes at 4 weeks and 20 weeks due to freeze–thaw cycles, (a) w/c ratio of 0.4, (b) w/c ratio of 0.5, and (c) w/c ratio of 0.6.

loss was more prominent in higher w/c ratio concrete mixes and at higher freeze–thaw cycles. According to Kisku et al. [53], the phenomenon of concrete strength loss during freeze–thaw cycles is attributed to the exposure of concrete to frost action before the development of desirable strength, the occurred expansion is associated with the formation of ice which leads to disruption and hence, irreparable strength loss. At the end of the 20th freezing and thawing cycles, all the concrete specimens endured higher compressive strength loss compared to the 4 weeks strength loss.

The highest strength losses at the end of the freezing and thawing cycles were exhibited by the RAC2 specimens. All the treated RAC specimens were able to minimize the strength losses of the untreated RAC. The best-performed treatment in terms of enhancing the frost resistance of untreated RAC was for the SCP + SE mixes. The higher reduction observed in the strength of the RAC specimen is mainly ascribed to the inner cracks evolved in the cement paste and the ITZ, which loosened the paste and weakened the bond between the aggregates and the cement paste. Kazmi et al. [51] stated that the higher strength loss in RAC compared to NAC after freezing and thawing cycles could be the results of many factors, i.e., higher water absorption of RA, mineralogical types of aggregates, higher porosity of RAC, w/c ratio, and air content.

The improved frost resistance of the SCP mixes is mainly attributed to the formation of a thin coating film of pozzolanic powder around the RA surface that occupied all the pores and reduced the high water absorption of RA [23]. The reduction in strength and mass loss of the SE mixes can be ascribed to the use of this batching technique (SE) which stems from allowing the sand particles in the mixture to mix more readily with water and cement, thus reducing the water absorbed by the RA. This is in line with the work of Liang et al. [25] who reported improved properties of the untreated RAC after using the SE mixing method.

5.3. Effects of SCP and SE on sulphate resistance of RACs

5.3.1. Visual inspection

Fig. 7 shows some of the test specimens after 20 weeks of exposure to sulphate attack. The results of the visual inspection for any physical change to the test specimens showed that there were no observed changes in terms of expansion in dimension or any spalling in any of the test specimens after immersing in sodium sulphate solution for 20 weeks. Crystallized salt and efflorescence were observed covering the upper surface of the test specimens after exposure to the sulphate environment. The degree of the crystallized salt was observed to increase with increased time of immersion in a sulphate solution.

5.3.2. Mass change due to sulphate attack

The results of the mass change rate of the NAC1, RAC2, SCP, SE, SCP + SE concrete specimens under sulphate attack for 20 weeks are shown in Fig. 8.

The results showed a general trend of mass increase for all the concrete specimens after exposure to sulphate solution at all w/c ratios. This is due to the formed ettringite within the concrete structure that causes internal stresses that leads to the loss of strength. Ettringite formed as the result of the occurred reaction between the hydrated cement products and the sulphate ions in the sulphate solutions, leading to the production of gypsum. This produced gypsum converts the tricalcium aluminate (C_3A) to ettringite [54,55]. It also can be indicated that an increase in w/c ratio and exposure time to sulphate attack resulted in a mass gain increase for all the concrete specimens. This can be explained as the concentration of sulphate within concrete structure increasing with time during exposure and decreasing with the depth of concrete. The decrease in sulphate content with depth of concrete is because sulphate ions need to transfer to the interior structure of the unsaturated concrete by either diffusion, capillary sorption, and penetration [56].

The growth rate of sulphate concentration by penetration through the micropores in the first 4 weeks is low and slow because of the low water absorption of concrete, and then it increases with time, as the porosity of concrete decreases due to the occurred reaction between the sulphate ions and the hydrated cementitious products. The gypsum and ettringite formed in the micropores of concrete via this chemical reaction can delay the diffusion process during the first 4 weeks of sulphate exposure. Nonetheless, this diffusion process accelerates with time as a result of increased concrete porosity due to the generated micro-cracks because of the internal crystallisation pressure applied on the pore walls of concrete by the ettringite formed. Additionally, another reason that could accelerate the diffusion process is the leaching of calcium [57,58].

After 20 weeks of sulphate exposure, the NAC1 specimens exhibited the lowest mass gain across all the concrete specimens, whilst the untreated RAC2 specimens endured the highest mass gain. This can be ascribed to the poor quality of RA compared to NA. RA is porous in nature, hence it absorbed a significant amount of water during mixing. This resulted in higher porosity of concrete which in turn leads to higher penetration of sulphate ion. Thus, higher uptake of gypsum and greater formation of ettringite was obtained, and ultimately greater damage to sulphate attack. This is in line with the results of Xie et al. [59] study, which showed that the mass gain of RACs increased slightly up to 0.69 % by 40 weeks of exposure to sulphate due to the ettringite and gypsum (expansion products) formed by the chemical reaction between the sulphate ions and the hydrated cement products.

All the enhanced RACs showed a lesser gain in mass and enhanced sulphate resistance after 20 weeks of exposure to sulphate, compared to the untreated RAC2 specimens. The enhanced sulphate resistance of the SCP specimens could be explained by the enhanced porosity due to the pozzolan coated layer formed around the RA surface that filled the micropores and the micro-cracks of RA. The enhanced resistance to sulphate attack of the SE specimens can be ascribed to the efficiency of the sand enveloped batching technique in reducing the water absorption of

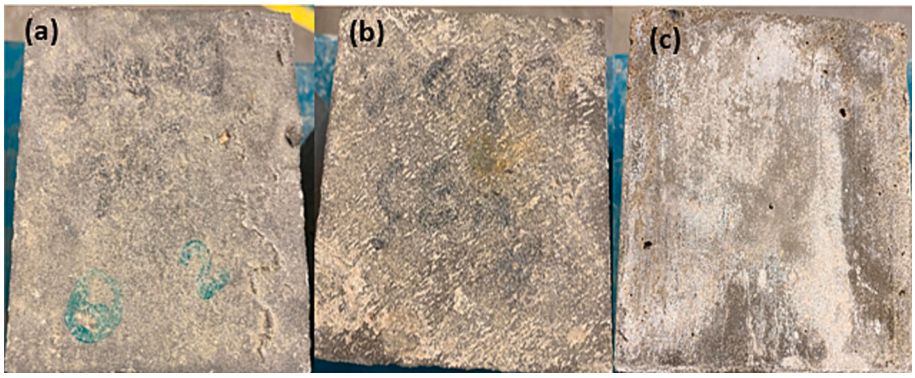

Fig. 7. Some of the test specimens after 20 weeks of exposure to sulphate, (a) NAC1 specimen, (b)SCP + SE specimen, (c) RAC2 specimen.

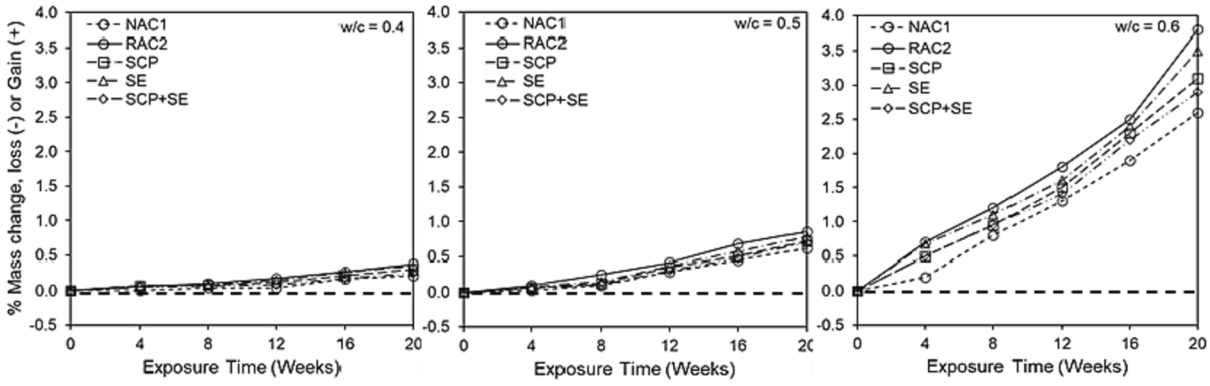

Fig. 8. Mass change (loss or gain) of the enhanced RACs due to sulphate attack.

RA during mixing, and hence strengthening the whole matrix [60]. Similarly, Kazmi et al. [61] reported lesser mass gain for treated RACs compared with untreated RACs, after 10 weeks of sulphate exposure.

5.3.3. *Strength loss due to sulphate attack*

Fig. 9 shows the residual compressive strength of the NAC1, the untreated RAC2, and the enhanced RACs after exposure to sulphate solution for up to 20 weeks.

Overall, all the test concrete specimens endured compressive strength loss after exposure to sulphate solution. The strength loss rate is higher at the end of the 20 weeks exposure at higher w/c ratios. None of the test concrete specimens showed a significant reduction in compressive strength after 4 weeks of exposure to sulphate solution except for the untreated RAC2 specimen. Xie et al. [59] examined the effects of sulphate attack on untreated recycled aggregate concrete for up to 40 weeks, the results showed that the RACs exposed to sulphate attack showed higher strength loss by 20 % compared RACs without sulphate, after 40 weeks of exposure time. In addition, the RACs started to exhibit a loss in strength after 22 weeks of exposure time. Xie et al. [59] explained these results as the internal pressure caused by the crystallisation of ettringite exceeded the tensile strength capacity of concrete, resulting in internal propagated microcracks and damage. All the treated RACs specimens showed a lesser reduction in the 4 weeks strength compared to the untreated RAC2 specimens. The combined treatments given in SCP + SE specimens showed the lowest reduction in compressive strength after 4 weeks of exposure time compared to the SE and SCP specimens.

After 20 weeks of immersion in sulphate solution, all the concrete specimens showed a higher reduction in compressive strength loss compared to the 4 weeks of sulphate attack. Amongst all the concrete specimens, the NAC1 specimens recorded the lowest loss in compressive strength after 20 weeks of exposure to sulphate solution, whereas the RAC2 specimens exhibited the highest strength loss. The results also indicated enhanced sulphate resistance achieved by the treated RACs in terms of strength loss after 20 weeks of sulphate exposure. The SCP + SE showed the lowest reduction in compressive strength after 20 weeks of exposure to sulphate. The enhanced sulphate resistance of the SCP specimens could be explained by the enhanced water absorption due to the pozzolan coated layer formed around the RA surface that filled the micropores and the micro-cracks of RA. The enhanced resistance to sulphate attack of the SE specimens can be attributed to the efficacy of the sand envelope batching technique in reducing the water absorption of RA during mixing, and hence densifying the whole matrix [60].

The literature shows that concrete under sulphate exposure exhibited a higher increase in its compressive strength up to 22 to 25 weeks compared to water cured concretes, and then the compressive strength tends to decrease rapidly at later ages of exposure to sulphate. Xie et al. [59] reported about a 10 % to 12 % higher increase in compressive strength for recycled aggregate concrete exposed to sulphate solution compared with concretes cured in water after 22 weeks of curing age. This higher increase in compressive strength can be ascribed due to the pore structure being filled by the expansion products. Nonetheless, this was not observed in the current study and this could be because the present study has only examined the compressive strength loss of the concrete test specimens after 4 weeks and 20 weeks of sulphate attack.

5.4. *Microstructure investigations*

Figs. 10 and 11 show the SEM images of the microstructure of NAC1 and untreated RAC2 samples, respectively.

The SEM observations for the NAC1 specimen revealed that the structure of the NAC1 is a well-formed, dense, and well-compacted structure of the aggregate-cement paste matrix, specifically at the interfacial zones. Whereas the SEM observations for the untreated RAC2 specimens show that the microstructure of the RAC2 specimen is quite different and complicated structure than that of the NAC1 specimen, due

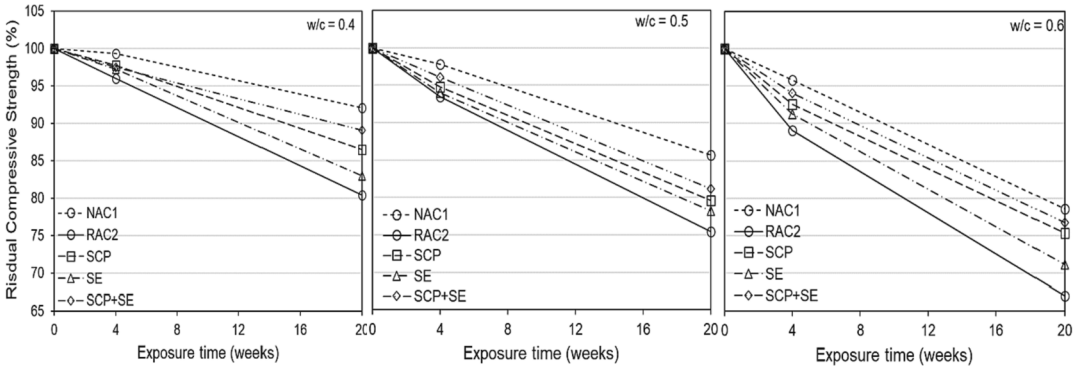

Fig. 9. Residual compressive strength of the treated RACs due to sulphate exposure.

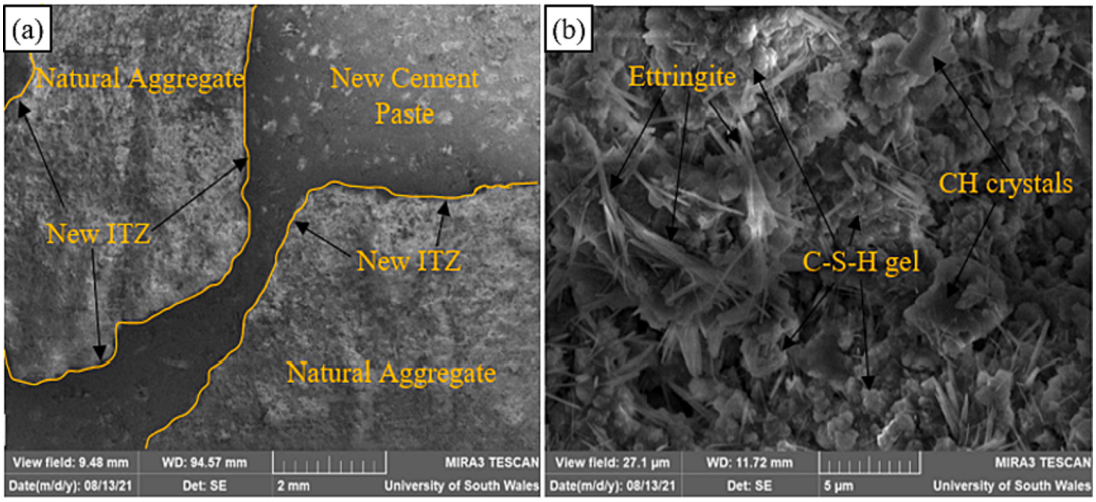

Fig. 10. SEM images of NAC1 sample, (a) microstructure of NAC1 sample, (b) SEM image for the hydrated compounds developed in NAC1 sample.

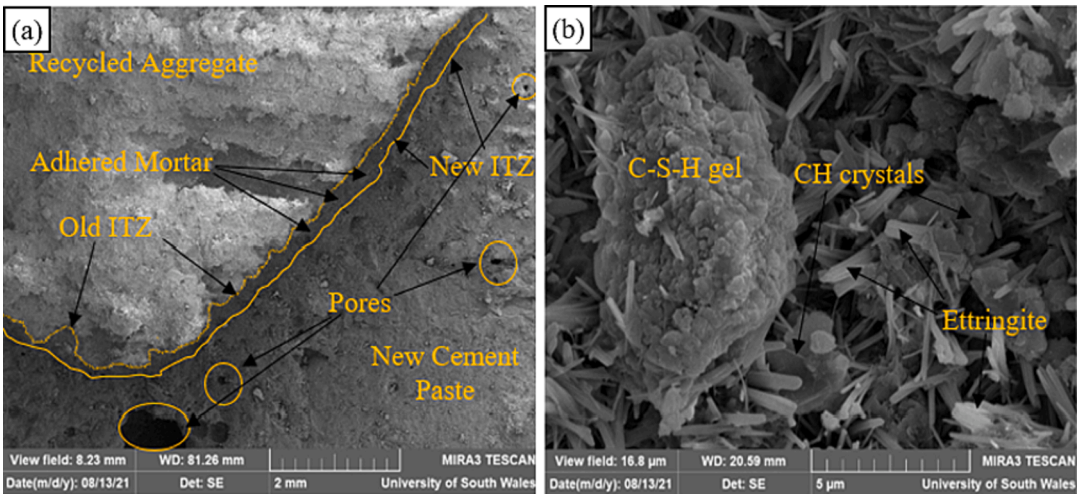

Fig. 11. SEM images of RAC2 sample, (a) microstructure of RAC2 sample, (b) SEM image for the hydrated compounds developed in RAC2 sample.

to the presence of the adhered mortar on the RA surface which leads to the formation of two interfacial transition zones (ITZ), the first one is between the RA (virgin aggregate) and the adhered mortar and another one between the adhered mortar and the new cement paste. This is in line with the studies of Poon et al. [62], Otsuki et al. [63], and Li et al. [64].

The SEM observation for the NAC1 specimen shows that the expansion of crack around the joint boundary between the NA and the cement paste indicates that the constructed cement paste in the designed mix possesses strong coherence and was able to withstand the target load, whilst the SEM observation for RAC2 specimen indicates the appearance of large pores, voids, cavities, and hollow spaces, as well as the presence of the clustered pores, and micro-cracks around the ITZ, indicating that the cement paste was not sufficiently compacted. These porous zones and cavities ultimately weaken the bond between the aggregates and the cement paste, which may possibly explain the lowered strength of RAC2 specimens compared to the NAC1 specimen. Similar findings were observed by Poon et al. [62].

The old ITZ in the RAC plays a vital role in defining the quality of the RAC compared to the new ITZ. Otsuki et al. [63] stated that at high water to cement ratios, if the characteristics of the old ITZ are better than the new ITZ, the strength of the RAC is comparable to the of NAC, whilst at low water to cement ratios, a weaker old ITZ results in lower strength of RAC compared to NAC. According to Xiao et al. [65], an increase in the ratio of the mechanical properties of the old ITZ (i.e., elastic modulus and strength), leads to higher strength but reduced ductility. Nonetheless, the new ITZ was found to have minimal effects on the properties of the RAC.

Accordingly, it can be seen that the old ITZ forms the weakest link in the RAC matrix and results in a more fragile microstructure of RAC due to its porous nature, weak bonding with the new cement paste, the presence of the loose particles, voids, pores, and micro-cracks [66]. In addition, the adhered mortar has a lower modulus of elasticity than that of the RA, which results in a lower modulus of elasticity of the RAC compared to NAC [63].

The characteristics of ITZ are governed by the quality of the adhered mortar, and the type of aggregate, as it was found to be thicker and better for recycled limestone aggregate than recycled gravel aggregate [65]. It was argued that the old ITZ acts as the weakest link that limits the strength phase in RAC as it forms a barrier wall between the cement paste phase and the RA phase within concrete. It also prevents transferring the loads as the cracks develop first near the ITZ [63].

Poon et al. [62] pointed out that the ITZ acts as a gradual transition zone in which its thickness is influenced by the degree of hydration and the content of the adhered mortar on the RA surface. Behera et al. [67] argued that the ITZ is highly porous and consists of less unhydrated products, a higher concentration of calcium hydroxide, and ettringite. Behera et al. [67] pointed out that the ITZ is comprised of numerous

minute intrinsic pores, voids, micro-cracks, and fissures.

According to Thomas et al. [44] and Xiao et al. [65], the porous nature of ITZ leads to lower strength and reduced modulus of elasticity around the surrounded cement paste matrix. The authors added that owing to the very poor microstructure of ITZ, the RAC stiffness is lowered and does not withstand the transferred stresses. Khalaf & DeVenny [68] argued that the cement paste can only partially penetrate the RA surface due to the variation in sizes of the existing pores and cracks on the RA surface, however, water can easily penetrate these pores which explains the higher water absorption of RA.

Khalaf & DeVenny [68] also stated that several fine flake-like and whisker-like crystals were observed in the pores and voids of the ITZ. Behera et al. [67] revealed that the formed incomplete hydration calcium hydroxide crystals attached to the surface of the RA lead to the development of a highly porous structure in the ITZ as a result of the accumulation of water film in the surrounding area to the RA surface. This may explain the poor durability performance of the RAC2 specimen, as it is associated with the porous nature of RA, the higher absorption capacity, and the poor ITZ.

Le & Bui [43] observed that there is a gradient of porosity in the ITZ zone, and this porosity increases from the cement paste to the RA surface. The reason behind this complicated microstructure can be explained as follows, as the water content increases and the cement content decreases, at the boundary of the RA. It was also observed that this zone initial thickness is several dozens of microns. During the curing phase, the thickness of the ITZ decreases due to the reduced porosity as a result of the formed hydrated products. In addition, during this phase, a transmission of hydration products occurs between the new cement paste and the adhered mortar [68]. Figs. 12, 13, and 14 show the SEM images of the SE concrete sample, the SCP concrete sample, and the SCP + SE concrete sample, respectively.

The SEM observations for the SE specimen in Fig. 12 showed a better-compacted structure of RAC. It also showed fewer cracks and lesser pores around the ITZ due to the coated RA with the sand-rich mortar during the initial stage of mixing. The literature showed limited studies on the microstructure investigations of RAC produced with sand enveloped mixing approach, nonetheless, Jagan et al. [69] studied the effects of mixing RAC using sand enveloped mixing approach on the microstructure of RAC. The results of the SEM investigations showed that the microstructure of RAC was enhanced with lesser cracks and pores and better bonding behaviour due to the non-porous stiff sand-rich mortar that was produced in the early stage of the mixing process which covered the RA surface.

The SEM observations for the SCP specimen in Fig. 13 showed that the ITZ was much tighter and more compact, the width and number of the micro-cracks were reduced, and the cement paste was relatively denser, compared to the untreated RAC2 specimen. It was also observed that the number of pores and voids was reduced which reflects on the reduced porosity, which was possibly related to the larger amount of calcium silicate hydrates and calcium hydroxide products that filled the pores and the micro-cracks.

The possible reasons behind the microstructure enhancement of RAC (SCP specimen) with treated RA by coating with cement-PFA + SF solution are as follow, (i) the relatively lower water to binder ratio of coated layer on the RA surface leads to denser and stronger ITZ, thus higher strength of RAC, (ii) the use of micro-fillers SF and PFA tend to flocculate due to their overwhelming specific area and better packing density, (iii) the coated cement- pozzolan layer on the RA surface forms a barrier that reduces inner bleeding of water, (iv) and the incorporation of the treated RA in RAC limits the amount of the absorbed effective mixing water during mixing. This is in line with the study of Wang et al. [49] who treated RA with cement and fly ash slurry and the results of the SEM observations still showed the presence of micro-cracks and pores at the ITZ zone, but the micro-cracks were much smaller compared to the untreated RAC specimen. The authors added that the new ITZ was filled with overlaid hydration products, the micro-cracks got disappeared and the ITZ was enhanced.

The SEM images for the SCP + SE specimen in Fig. 14 showed the best enhanced higher quality microstructure compared to SCP and SE specimens. This is the result of the synergetic effects of soaking RA in cement-pozzolan solution followed by mixing using sand enveloped mixing approach. The SCP + SE specimen showed the fewest cracks and pores and the densest ITZ. In addition, the microstructure of the SCP + SE specimen achieved excellent compaction, and highly strengthened ITZ with excellent interlock and bonding between the RA and the cement paste.

The findings of the microstructue investigations support and validate the durability test results which demonstrated that the SCP + SE mixes achieved the highest enhancements in water absorption, freeze–thaw resistance, and sulphate attack. It is worth noting that, no study in the literature examined the microstructure investigations of RAC produced with treated RA by soaking in cement-PFA + SF solution combined with sand enveloped mixing approach.

6. Cost analysis

Several factors play significant role in promoting the use of recycled aggregate in the construction industry in comparison with natural aggreagte. These are cost effiecney, environemental impact, performance, sustainability, and durability. Table 7 shows the price breakdown per concrete mix. It is clearly notable that the untreated RAC mix have a lower carbon footprint and lower price per cubic meter compared to NAC. Nevertheless, based on the durability performance in this study, the untreated RAC exhbitied poor durability properties compared to NAC. Therefore, there was a need to carry out treatment/ enhancement methods in order to enhance the quality of RAC. However, several

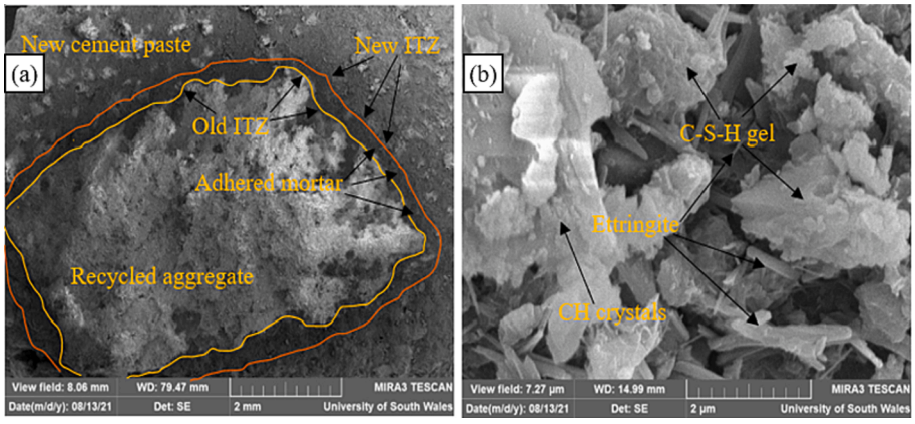

Fig. 12. SEM images for SE sample, (a) microstructure of SE sample, (b) SEM image for the hydrated compounds developed in SE sample.

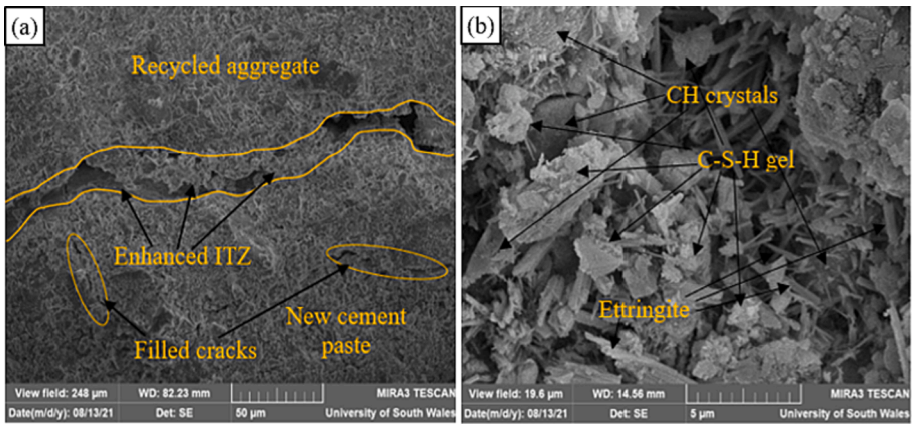

Fig. 13. SEM images for SCP sample, (a) microstructure of SCP sample, (b) SEM image for the hydrated compounds developed in SCP sample.

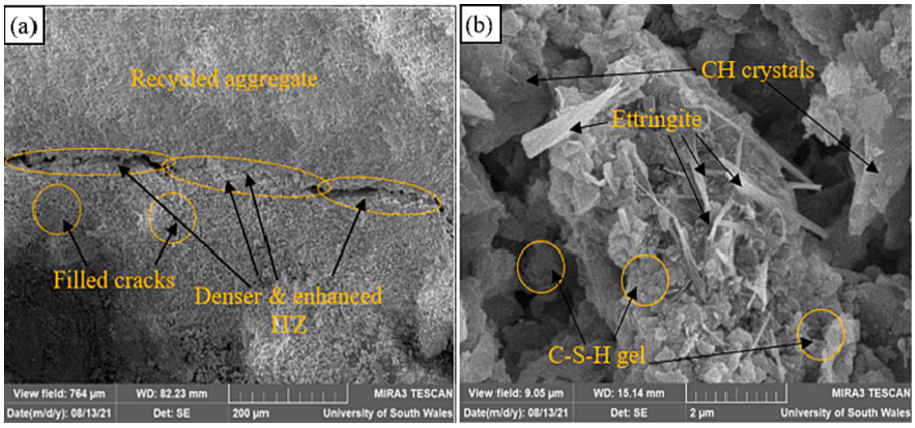

Fig. 14. SEM images for SCP + SE sample, (a) microstructure of SCP + SE sample, (b) SEM image for the hydrated compounds developed in SCP + SE sample.

Table 7
Price breakdown of the different concrete mixes and the associated embodied carbon dioxide footprint.

Mix	Constituent						Concrete cost (£/m^3) [a]	Cost /NAC1	Cost/ RAC2	kg CO_2e / m^3 concrete[b]
	OPC	PFA	SF	NA	Sand	RA				
Estimated Price (£/t)	150	650	550	40	40	15	–	–	–	–
NAC1 (£/m^3)	67	–	–	58	27	–	152	100 %	–	450
RAC2 (£/m^3)	67	–	–	–	27	19	113	74 %	100 %	437
SCP (£/m^3)	83	48	41	–	27	19	218	143 %	193 %	530
SE (£/m^3)	67	–	–	–	27	19	113	74 %	100 %	437
SCP + SE (£/m^3)	83	48	41	–	27	19	218	143 %	193 %	530

[a] Tentative price for each concrete ingredient including SF and PFA were obtained from searching through trading local suppliers.
[b] The estimated embodied carbon footprint was calculated based on the data given in [70] and excluding transportation.

factors should be considered when selecting the type of the enhancement methods. As shown in Table 7, soaking RA in cement-pozzalan solution prior to mixing (SCP mix) increased the cost and the associated carbon footprint of the end product by 93 % and 17 %, respectively, compared to the untreated RAC. In the contrary, the utilization of sand envelop batching technique (SE mix) kept the same cost and the same carbon footprint compared to the untreated RAC.

Fig. 15 shows the cost analysis of the various enhancement methods against different factors related to untreated RAC. It can be seen the use of bi-combination of enhancement methods (SCP + SE) obtained the best performance in terms of durability properties and compressive strength at 28-days. Nevertheless, the sole use of batching technique (SE) seemed a better choice in terms of other influencing factors such as cost efficiency, carbon dioxide footprint, simplicity, application time, and feasibility.

In view of this discussion, it is quite important to consider the cost-efficiency, sustainability, and efficiency of enhancement method for RA and RAC. Although treatments such as soaking RA in cement-pozzolan may increase the cost and CO_2 emission for RAC, it is still a better choice compared to other treatments utilized by other researchers [9]. To this end, in order to successfully promote the use of RA in the construction industry, several factors should be considered specifically the feasibility of the treatment method to be used in practice at bulk production.

7. Conclusions

Concrete with untreated recycled aggregate demonstrated low-quality durability performance compared to natural aggregate concrete due to several factors. Two of the main factors are the weak porous adhered mortar on the RA surface and the old weak interfacial transition zone which resulted in a weak interfacial transition zone and weak

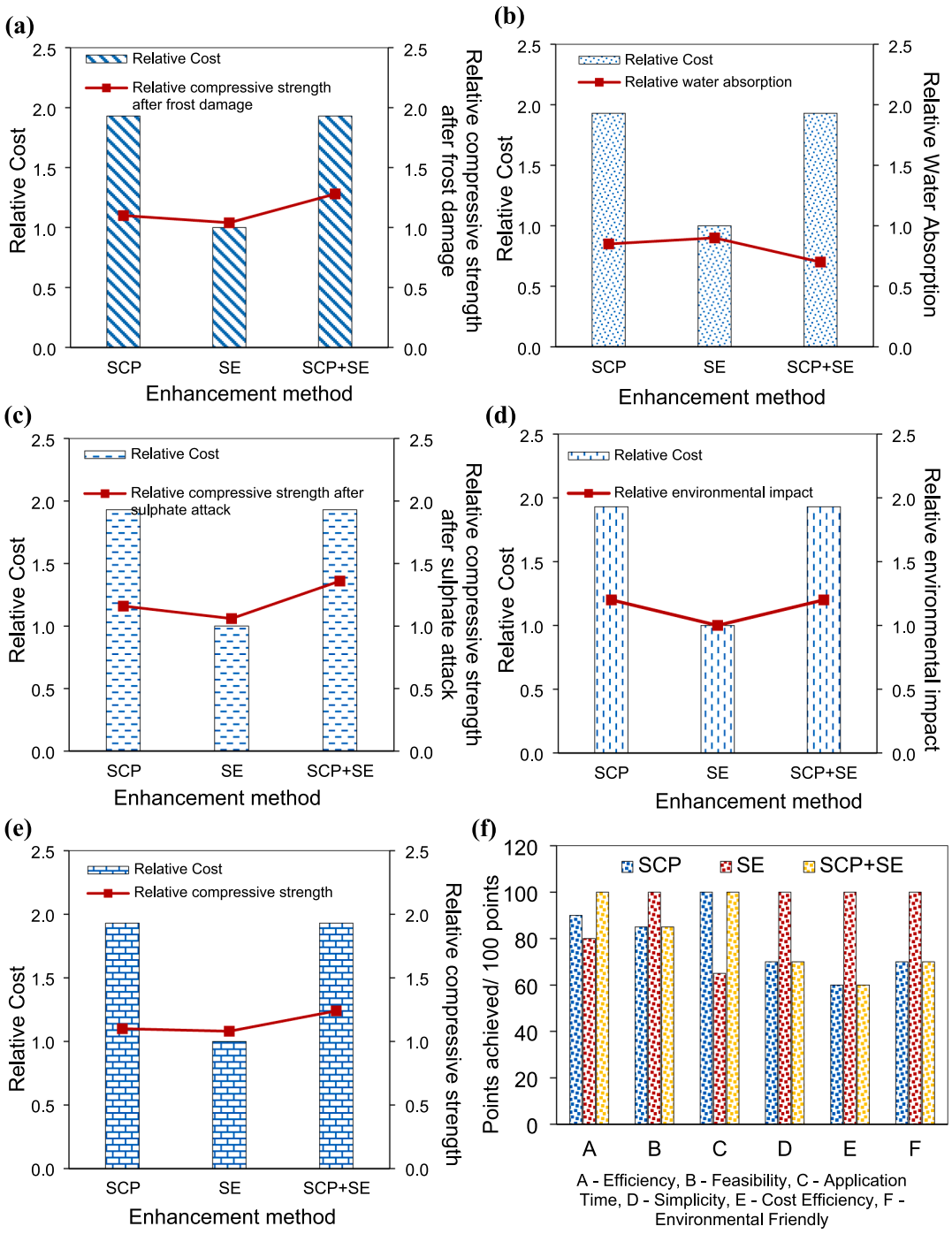

Fig. 15. Cost analysis of the various enhancement methods: (a) cost vs compressive strength after 20 cycles of freezing-thawing, (b) cost vs water absorption, (c) cost vs compressive strength after exposure to sulphate attack, (d) cost vs environmental impact, (e) cost vs 28-day compressive strength, (f) other influencing factors.

bonding within the recycled aggregate concrete matrix. Other concerns include variation in composition, previous loading, processing, and weathering compared to freshly crushed natural aggregates. This paper has presented laboratory-based investigations on the effects of different enhancement methods on the durability properties of concretes with untreated RA and treated RA. The following specific conclusions can be drawn:

1. ***Recycled aggregate concrete with untreated RA:*** RAC with untreated RA showed poor durability performance in terms of water absorption, resistance to freeze–thaw cycles, and sulphate attack compared to NAC. This was ascribed mainly to the lower quality of the untreated RA, the high-water absorption of the untreated RA, the presence of micro-pores, cavities, micro-cracks, and the poor quality of the old ITZ in the RAC with untreated RA. The microstructure of the RAC had two ITZs whereas the microstructure of the NAC had one ITZ. The SEM images have also indicated that the microstructure of the RAC with untreated RA was poorly compacted with obvious pores, cavities, microcracks, and weak bonding between the RA and the new cement paste.
2. ***Soaking RA in cement-PFA + SF solution (SCP):*** RAC with treated RA by the SCP method achieved enhanced water absorption compared to RAC with untreated RA. The SCP enhanced the resistance to freeze–thaw and sulphate attack showing reduced mass

losses/gains and lower strength losses compared to the untreated RAC. This was mainly due to the enhanced water absorption through the effects of the SCP treatment in filling and sealing the pores and the micro-cracks on the RA surface. The SEM images observed for the SCP specimen showed a better microstructure compared to the untreated RAC. The SCP specimen exhibited better-compacted microstructure, lesser pores and microcracks, denser ITZ, and better interlocking behaviour between the RA and the cement paste.

3. ***Sand envelope mixing approach (SE):*** the sole use of this batching technique also demonstrated enhanced water absorption, resistance to freezing-thawing, and enhanced resistance to sulphate attack. The enhancement observed in the durability properties of the SE mixe can be ascribed to the use of this batching technique (SE) which stems from allowing the sand particles in the mixture to mix more readily with water and cement. This resulted in covering the RA with premixed cement/ mortar slurry that filled up the cracks and pores of RAC, hence enhancing its resistance to water absorption and ultimately improving the durability performance. The sole use of the sand enveloped mixing approach has also led to a better compacted and formed microstructure, but the presence of the voids and microcracks was more evident compared to the SCP specimen.
4. ***Bi-combination of SCP + SE:*** the combination of treating RA by soaking in cement-PFA + SF solution followed by mixing using sand envelop batching technique achieved higher durability performance compared to the sole use of the SCP and SE methods. The combination of the SCP + SE treatment resulted in the most desired microstructure of the RAC. The synergetic effects of these two treatments led to a relatively stronger and compacted microstructure with the fewest pores and microcracks, stronger and denser ITZs.
5. ***Cost analysis:*** several factors may influence the selection of the best treatment methods. The efficiency, cost-effectiveness, feasibility, and the environmental impact are the most influence factors that should be carefully considered prior to application of any treatment.

Funding

This research did not receive any specific grant from funding agencies in the public, commercial, or non-profit sectors.

CRediT authorship contribution statement

Qusai Al-Waked: Conceptualization, Methodology, Validation, Investigation, Visualization, Writing – original draft, Writing – review & editing. **Jiping Bai:** Validation, Writing – review & editing, Supervision, Project administration. **John Kinuthia:** Validation, Writing – review & editing, Supervision, Project administration. **Paul Davies:** Validation, Writing – review & editing, Supervision, Project administration.

Declaration of Competing Interest

The authors declare that they have no known competing financial interests or personal relationships that could have appeared to influence the work reported in this paper.

Data availability

Data will be made available on request.

References

[1] Kim, J., 2022. Influence of quality of recycled aggregate on the mechanical properties of recycled aggregate concrete: An overview. Construction and Building Materials, Volume 328m P. 127071. https://doi.org/10.1016/j.conbuildmat.2022.127071.
[2] W. Lu, Big data analytics to identify illegal construction waste dumping: A Hong Kong study, Resour. Conserv. Recycl. 141 (2019) 264–272, https://doi.org/10.1016/j.resconrec.2018.10.039.
[3] V. Tam, M. Soomro, A. Evangelista, A review of recycled aggregate in concrete applications (2000–2017), Constr. Build. Mater. 172 (2018) 272–292, https://doi.org/10.1016/j.conbuildmat.2018.03.240.
[4] R. Silva, J. Brito, R. Dhir, Properties and composition of recycled aggregatesfrom construction and demolition waste suitable for concrete production, Constr. Build. Mater. 65 (2014) 201–217, https://doi.org/10.1016/j.conbuildmat.2014.04.117.
[5] V. Tam, Comparing the implementation of concrete recycling in the Australian and Japanese construction industries, J. Cleaner Prod. 17 (7) (2009) 688–702, https://doi.org/10.1016/j.jclepro.2008.11.015.
[6] A. Grabiec, D. Zawal, W. Rasaq, The effect of curing conditions on selected properties of recycled aggregate concrete, Appl. Sci. 10 (2020) 1–15, https://doi.org/10.3390/app10134441.
[7] H. Al Ajmani, F. Suleiman, I. Abuzayed, A. Tamimi, Evaluation of concrete strength made with recycled aggregate, Buildings 9 (2019) 1–14, https://doi.org/10.3390/buildings9030056.
[8] G.L. Vieira, J.Z. Schiavon, P.M. Borges, S.R. da Silva, J.J. de Oliveira Andrade, Influence of recycled aggregate replacement and fly ash content in performance of pervious concrete mixtures, J. Cleaner Prod. 271 (2020) 122665.
[9] A. Bahraq, J. Jose, M. Shameem, M. Maslehuddin, A review on treatment techniques to improve the durability of recycled aggregate concrete: Enhancement mechanisms, performance, and cost analysis, Journal of Building Engineering 55 (2022), 104713, https://doi.org/10.1016/j.jobe.2022.104713.
[10] M. Etxeberia, E. Vazquez, A. Mari, M. Barra, Influence of amount of recycled coarse aggregates and production process on properties of recycled aggregate concrete, Cem. Concr. Res. 37 (5) (2007) 735–742, https://doi.org/10.1016/j.cemconres.2007.02.002.
[11] H. Guo, C. Shi, X. Guan, J. Zhu, Y. Ding, T.-C. Ling, H. Zhang, Y. Wang, Durability of recycled aggregate concrete - A review, Cem. Concr. Compos. 89 (2018) 251–259.
[12] Al-Bayati, H., Das, P., Tighe, S. & Baaj, H., 2016. Evaluation of various methods for enhancing the physical and morphological properties of coarse recycled concrete aggregate. Construction and Building Materials, Volume 112, pp. 284-298, https://doi.org/ 10.1016/j.conbuildmat.2016.02.176.
[13] K. Bru, S. Touzé, F. Bourgeois, N. Lippiatt, Y. Ménard, Assessment of a microwave-assisted recycling process for the recovery of high-quality aggregates from concrete waste, Int. J. Miner. Process. 126 (2014) 90–98.
[14] A. Gonzalez-Corominas, M. Etxeberria, Properties of high-performance concrete made with recycled fine ceramic and coarse mixed aggregates, Constr. Build. Mater. 68 (2014) 618–626, https://doi.org/10.1016/J.CONBUILDMAT.2014.07.016.
[15] S. Kou, C. Poon, Enhancing the durability properties of concrete prepared with coarse recycled aggregate, Constr. Build. Mater. 35 (2012) 69–76, https://doi.org/10.1016/j.conbuildmat.2012.02.032.
[16] A. Grabiec, J. Klama, D. Zawal, D. Krupa, Modification of recycled concrete aggregate by calcium carbonate bio-deposition, Constr. Build. Mater. 34 (2012) 145–150, https://doi.org/10.1016/j.conbuildmat.2012.02.027.
[17] J. Chen, J. Thomas, H. Jennings, Decalcification shrinkage of cement paste, Cem. Concr. Res. 36 (5) (2006) 801–809, https://doi.org/10.1016/j.cemconres.2005.11.003.
[18] W. Shaban, J. Yang, H. Su, K. Mo, J. Li, J. Xie, Quality Improvement Techniques for Recycled concrete Aggregate: A review, J. Adv. Concr. Technol. 17 (2019) 151–167, https://doi.org/10.3151/jact.17.151.
[19] S. Kou, B. Zhan, C. Poon, Use of a CO2 curing step to improve the properties of concrete prepared with recycled aggregates, Cem. Concr. Compos. 45 (2014) 22–28, https://doi.org/10.1016/j.cemconcomp.2013.09.008.
[20] J. Li, H. Xiao, Y. Zhou, Influence of coating recycled aggregate surface with pozzolanic powder on properties of recycled aggregate concrete, Constr. Build. Mater. 23 (3) (2009) 1287–1291, https://doi.org/10.1016/j.conbuildmat.2008.07.019.
[21] V. Tam, C. Tam, Y. Wang, Optimization on proportion for recycled aggregate in concrete using two-stage mixing approach, Constr. Build. Mater. 21 (10) (2007) 1928–1939, https://doi.org/10.1016/j.conbuildmat.2006.05.040.
[22] Liang, Y., Ye, Z., Vernerey, F. & Xi, Y., 2015. Development of processing methods to improve strength of concrete with 100% recycled coarse aggregate. *Journal of Materials in Civil Engineering*, 27(5), p. 130801045339002, http://doi.org/10.1061/(ASCE)MT.1943-5533.0000909.
[23] S. Kazmi, M. Munir, Y.-F. Wu, I. Patnaikuni, Y. Zhou, F. Xing, Effect of recycled aggregate treatment techniques on the durability of concrete: A comparative evaluation, Constr. Build. Mater. 264 (2020), 120284, https://doi.org/10.1016/j.conbuildmat.2020.120284.
[24] Q. Al-Waked, J. Bai, J. Kinuthia, P. Davies, Enhancing the aggregate impact value and water absorption of demolition waste coarse aggregates with various treatment methods, Case Stud. Constr. Mater. 17 (2022) e01267.
[25] British Standards Institution, BS EN 12620:2002+A1:2008—Aggregates for Concrete, London, UK, British Standards Institution, 2008.
[26] British Standards Institution, BS EN 13242:2013—Aggregates for unbound and hydraulically bound materials for use in civil engineering work and road construction, London, UK, British Standards Institution, 2013.
[27] Derwen, 2016. Recycled Aggregate. [Online] Available at: https://www.derwengroup.co.uk [Accessed 10 Feburary 2022].
[28] British Standards Institution. BS 8500-2:2015 +A2: 2019—Concrete-Complementary British Standard to BS EN 206. Part 2: Specification for constituent materials and concrete; British Standards Institution: London, UK, 2019.
[29] British Standards Institution. BS EN 933-1:2012—Tests for geometrical properties of aggregates. Part 1: Determination of particle size distribution—Sieving method; British Standards Institution: London, UK, 2012.

[30] M.J. Munir, S.M.S. Kazmi, Y.-F. Wu, I. Patnaikuni, J. Wang, Q. Wang, Development of a unified model to predict the axial stress–strain behavior of recycled aggregate concrete confined through spiral reinforcement, Eng. Struct. 218 (2020) 110851.
[31] British Standards Institution. BS EN 933-3: 2012—Tests for geometrical properties of aggregates. Part 3: Determination of particle shape—Flakiness index; British Standards Institution: London, UK, 2012.
[32] British Standards Institution. BS EN 933-4:2008—Tests for Geometrical Properties of Aggregates. Part 4: Determination of Particle Shape—Shape Index; British Standards Institution: London, UK, 2008.
[33] British Standards Institution. BS EN 1097-6:2013—Tests for Mechanical and Physical Properties of Aggregates. Part 6: Determination of Particle Density and Water Absorption; British Standards Institution: London, UK, 2013.
[34] British Standards Institution. BS EN 1097-2:2020—Tests for mechanical and physical properties of aggregates. Part 2: Methods for determination of resistance to fragmentation; British Standards Institution: London, UK, 2020.
[35] British Standard Institution. BS EN 197-1:2011 - Cement. Composition, specifications and conformity criteria for common cements; British Standard Institution: London, UK, 2011.
[36] British Standard Institution. BS EN 450-1:2012 – Fly ash for concrete. Part 1: Definition, specifications and conformity criteria; British Standard Institution: London, UK, 2012.
[37] British Standard Institution. BS EN 13263-2:2005+A1:2009 – Silica fume for concrete. Part 2: conformity evaluation; British Standard Institution: London, UK, 2009.
[38] British Standards Institution. BS EN 206:2013+A1:2016: Concrete. Specification, performance, production and conformity; British Standards Institution: London, UK, 2016.
[39] British Standards Institution, BS EN 12390–2:2009: Testing hardened concrete, London, UK, Making and curing specimens for strength tests; British Standards Institution, 2009.
[40] Pd cen, ts, 12390–9. Testing hardened concrete. Part 9: Freeze-thaw resistance with de-icing salts -, Scaling. (2016).
[41] British Standards Institution, BS 1881–122:2011+A1:2020: Testing concrete, London, UK, Method for determination of water absorption; British Standards Institution, 2020.
[42] British Standards Institution. BS EN 206:2013+A2:2021: Concrete. Specification, performance, production and conformity; British Standards Institution: London, UK, 2021.
[43] H.-B. Le, Q.-B. Bui, Recycled aggregate concretes - A state-of-the-art from the microstructure to the structural performance, Constr. Build. Mater. 257 (2020), 119522, https://doi.org/10.1016/j.conbuildmat.2020.119522.
[44] C. Thomas, J. Setien, J. Polanco, P. Alaejos, M. Juan, Durability of RAC, Constr. Build. Mater. 40 (2013) 1054–1065, https://doi.org/10.1016/j.conbuildmat.2012.11.106.
[45] S. Lotfi, M. Eggimann, E. Wagner, R. Mroz, J. Deja, Performance of RAC based on a new concrete recycling technology, Constr. Build. Mater. 95 (2015) 243–256, https://doi.org/10.1016/j.conbuildmat.2015.07.021.
[46] F. Debieb, L. Courard, S. Kenai, R. Degimbre, Roller compacted concrete with contaminated RAs, Constr. Build. Mater. 23 (11) (2010) 3382–3387, https://doi.org/10.1016/j.conbuildmat.2009.06.031.
[47] W.H. Kwan, M. Ramli, K.J. Kam, M. Sulieman, Influence of the amount of recycled coarse aggregate in concrete design and durability properties, Constr. Build. Mater. 26 (2012) 565–573, https://doi.org/10.1016/j.conbuildmat.2011.06.059.
[48] V. Tam, C. Tam, K. Le, Removal of cement mortar remains from recycled aggregate using pre-soaking approaches, Resources, Conservation, and Recycled 50 (1) (2007) 82–101, https://doi.org/10.1016/j.resconrec.2006.05.012.
[49] B. Wang, L. Yan, Q. Fu, B. Kasal, A Comprehensive Review on Recycled Aggregate and Recycled Aggregate Concrete, Resour. Conserv. Recycl. 171 (2021), 105565, https://doi.org/10.1016/j.resconrec.2021.105565.
[50] R. Salem, E. Burdette, N. Jackson, Resistance to freezing and thawing of recycled aggregate concrete, ACI Mater. J. 1100 (3) (2003) 216–221.
[51] S. Kazmi, M. Munir, Y. Wu, I. Patnaikuni, Y. Zhou, F. Xing, Effect of different aggregate treatment techniques on the freeze-thaw and sulfate resistance of recycled aggregate concrete, Cold Reg. Sci. Technol. 178 (2020) 103–126, https://doi.org/10.1016/j.coldregions.2020.103126.
[52] C.-R. Wu, Y.-G. Zhu, X.-T. Zhang, S.-C. Kou, Improving the properties of recycled concrete aggregate with bio-deposition approach, Cem. Concr. Compos. 94 (2017) 248–254, https://doi.org/10.1016/j.cemconcomp.2018.09.012.
[53] N. Kisku, H. Joshi, M. Ansari, S.K. Panda, S. Nayak, S.C. Dutta, A critical review and assessment for usage of recycled aggregate as sustainable construction material, Constr. Build. Mater. 131 (2017) 721–740.
[54] W. Mullauer, R. Beddoe, D. Heinz, Sulphate attack expansion mechanisms, Cem. Concr. Res. 52 (2013) 208–215, https://doi.org/10.1016/j.cemconres.2013.07.005.
[55] J. Bizzozero, C. Gosselin, K. Scrivener, Expansion mechanisms in calcium aluminate and sulfoaluminate systems with calcium sulfate, Cem. Concr. Res. 56 (2014) 190–202, https://doi.org/10.1016/j.cemconres.2013.11.011.
[56] X. Zuo, W. Sun, C. Yu, Numerical investigation on expansive volume strain in concrete subjected to sulfate attack, Constr. Build. Mater. 36 (4) (2012) 404–410, https://doi.org/10.1016/j.conbuildmat.2012.05.020.
[57] R. Euml, L. Tixier, B. Mobasher, Modeling of damage in cement-based materials subjected to external sulfate attack. I: formulation, J. Mat. Civil Eng. 15 (4) (2003) 305–313, https://doi.org/10.1061/(ASCE)0899-1561(2003)15:4(305).
[58] Rozière, E., loukili, A., El Hachem, R. & Grondin, F., 2009. Durability of concrete exposed to leaching and external sulphate attack. *Cement and Concrete Research,* 39 (12), pp. 1188-1198. https://doi.org/10.1016/j.cemconres.2009.07.021.
[59] F. Xie, J. Li, G. Zhao, G. Zhou, H. Zheng, Experimental study on performance of cast-in-situ recycled aggregate concrete under different sulfate attack exposures, *Const.* Build. Mater. 253 (2020), 119144, https://doi.org/10.1016/j.conbuildmat.2020.119144.
[60] J. Wang, B. Vandevyvere, S. Vanhessche, J. Schoon, N. Boon, N. De Belie, Microbial carbonate precipitation for the improvement of quality of recycled aggregates, J. Cleaner Prod. 156 (2017) 355–366.
[61] S. Kazmi, M. Munir, Y. Wu, I. Patnaikuni, Y. Zhou, F. Xing, Influence of different treatment methods on the mechanical behavior of recycled aggregate concrete: a comparative study, Cem. Concr. Compos. 104 (2019), 103398, https://doi.org/10.1016/j.cemconcomp.2019.103398.
[62] C. Poon, Z. Shui, L. Lam, Effect of microstructure of ITZ on compressive strength of concrete prepared with RAs, Constr. Build. Mater. 18 (6) (2004) 461–468, https://doi.org/10.1016/j.conbuildmat.2004.03.005.
[63] N. Otsuki, S. Miyazato, W. Yodsudjai, Influence of recycled aggregate on interfacial transition zone, strength chloride penetration and carbonation of concrete, J. Mater. Civ. Eng. 15 (5) (2003) 443–451, https://doi.org/10.1061/(ASCE)0899-1561(2003)15:5(443).
[64] W. Li, J. Ziao, Z. Sun, S. Kawashima, S. Shah, Interfacial transition zones in RAC with different mixing approaches, Constr. Build. Mater. 35 (2012) 1045–1055, https://doi.org/10.1016/j.conbuildmat.2012.06.022.
[65] J. Xiao, W. Li, Y. Fan, X. Huang, An overview of study on recycled aggregate concrete in China (1996–2011), Constr. Build. Mater. 31 (2013) 364–383, https://doi.org/10.1016/j.conbuildmat.2011.12.074.
[66] S. Nayak, S.C. Dutta, A critical review and assessment for usage of recycled aggregate as sustainable conctruction material, Constr. Build. Mater. (2017) 721–740, https://doi.org/10.1016/j.conbuildmat.2016.11.029.
[67] M. Behera, et al., Recycled aggregate from C&D waste & its use in concrete - A breakthrough towards sustainability in construction sector: A review, Constr. Build. Mater. 68 (2014) 501–516, https://doi.org/10.1016/j.conbuildmat.2014.07.003.
[68] K. Kjellsen, O. Wallevik, L. Fjalberg, Microstructure and microchemistry of the paste-aggregate interfacial transition zone of high-performance concrete, Advance in Cement Research 10 (1998) 33–40, https://doi.org/10.1680/adcr.1998.10.1.33.
[69] S. Jagan, T. Neelakantan, P. Saravanakumar, Mechanical properties of recycled aggregate concrete surface treated by varation in mixing approaches, Journal of Construction 20 (2) (2021) 236–249, https://doi.org/10.1108/wje-02-2021-0089.
[70] Ice, November 10), Retrieved from, Concrete Embodied Carbon Footprint Calculator, 2019. Circular ecology: https://www.circularecology.com/embodied-carbon-footprint-database.html.